The FADE mass-stat

The FADE mass-stat: A technique for inserting or deleting particles in molecular dynamics simulations

Matthew K. Borg,[1,a)] Duncan A. Lockerby,[2,b)] and Jason M. Reese[3,c)]
[1]*Department of Mechanical and Aerospace Engineering, University of Strathclyde, Glasgow G1 1XJ, United Kingdom*
[2]*School of Engineering, University of Warwick, Coventry CV4 7AL, United Kingdom*
[3]*School of Engineering, University of Edinburgh, Edinburgh EH9 3JL, United Kingdom*

(Received 4 November 2013; accepted 28 January 2014; published online 20 February 2014)

The emergence of new applications of molecular dynamics (MD) simulation calls for the development of mass-statting procedures that insert or delete particles on-the-fly. In this paper we present a new mass-stat which we term FADE, because it gradually "fades-in" (inserts) or "fades-out" (deletes) molecules over a short relaxation period within a MD simulation. FADE applies a time-weighted relaxation to the intermolecular pair forces between the inserting/deleting molecule and any neighbouring molecules. The weighting function we propose in this paper is a piece-wise polynomial that can be described entirely by two parameters: the relaxation time scale and the order of the polynomial. FADE inherently conserves overall system momentum independent of the form of the weighting function. We demonstrate various simulations of insertions of atomic argon, polyatomic TIP4P water, polymer strands, and C_{60} Buckminsterfullerene molecules. We propose FADE parameters and a maximum density variation per insertion-instance that restricts spurious potential energy changes entering the system within desired tolerances. We also demonstrate in this paper that FADE compares very well to an existing insertion algorithm called USHER, in terms of accuracy, insertion rate (in dense fluids), and computational efficiency. The USHER algorithm is applicable to monatomic and water molecules only, but we demonstrate that FADE can be generally applied to various forms and sizes of molecules, such as polymeric molecules of long aspect ratio, and spherical carbon fullerenes with hollow interiors. © *2014 AIP Publishing LLC*. [http://dx.doi.org/10.1063/1.4865337]

I. INTRODUCTION

Molecular Dynamics (MD) simulations of fluids are typically categorised by their statistical ensemble. The two common ensembles are the constant-N, V, E (microcanonical) and the constant-N, V, T (canonical).[1] What this means is that in any MD simulation the number of molecules N in the system, the domain volume V, and the total energy E or temperature T remain unequivocally constant. There are several applications in various disciplinary fields, however, where the transfer of mass in MD simulations (i.e., a change in N) is of great practical importance, yet may not necessarily fit within well-established ensembles.

Our main interests, which have motivated us to develop the mass-stat method described in this paper, lie in the following applications. Concurrent hybrid techniques that couple molecular dynamics to a continuum model (such as the Navier-Stokes equations) require continuous exchange of hydrodynamic conservative properties, such as mass flux in time-varying problems,[2–4] or thermodynamic state properties such as mass density.[5] In addition, pure MD simulations may be of "open-systems," i.e., in which periodicity is no longer applicable.[6–9] For example, non-periodic flow over nanoscale objects such as carbon nanotubes,[10] localised dynamics of proteins in a solvent,[11] convective, specie-mixing, and thermal flows in nanoscale channel geometries;[5,12] and nanofiltration of water in pressure driven flows through nanotube membranes.[13] In all these examples there is a need for an efficient, robust method to insert and delete molecules on-the-fly within MD simulations.

A class of popular methods for performing particle insertions/deletions is in the constant-μ, V, T (grand canonical) ensemble, where μ is the chemical potential. In these grand canonical molecular dynamics (GCMD) simulations, MD is coupled with a Monte Carlo (MC) method, to inherit the best of the two approaches: the non-equilibrium time-dependent characteristics of MD, with the stochastic insertion/deletion control capability of MC at a target μ. In extended GCMD,[14–17] the domain is entirely described by both MD and MC descriptions, and N is modified from a real number into a continuously varying parameter, whose fractional part is included in the Hamiltonian of the system. In dual control-volume GCMD simulations,[18–20] MC volumes are applied only at two reservoir regions of a confined channel flow problem; for example, where the overlaying MD reservoirs are set at different chemical potentials.

The development of mechanical-type particle insertion techniques in MD is considerably simpler, enabling reasonable insertion rates in dense fluids at a computational efficiency that is sometimes better than an incorporated MC coupling. However, to date, these methods have been limited in

a)Electronic mail: matthew.borg@strath.ac.uk
b)Electronic mail: duncan.lockerby@warwick.ac.uk
c)Electronic mail: jason.reese@ed.ac.uk

number. A random approach to inserting particles, for example, is far from ideal in MD, because of the high probability of introducing simulation blow-up,[21] owing to the steep intermolecular potentials that exist between tightly packed molecules. In a random-placement method, blow-up can be avoided by checking the proximity of the inserted molecule to neighbouring molecules and repeating the search if, for example, it is placed too close to another molecule.[22] While it is not very clear how to determine a correct minimum separation that minimises spurious energy changes, the main drawbacks with this approach lies in dense fluids, which produce highly inefficient and expensive searches. The USHER protocol[23,24] has elegantly addressed these problems. In fact, owing to its simplicity, superior insertion rate and computational efficiency, USHER is the most current popular technique (from a mechanical perspective) for particle insertions in dense fluid simulations.

As the name suggests, USHER guides new molecules within an existing molecular configuration, using a steepest-descent scheme (similar to a Newton-Raphson method) within the local potential energy landscape. Only when a site at the prescribed value of potential energy is found, is the new molecule inserted. The target potential energy is generally chosen to be either the measured mean local potential energy per molecule (to maintain the same local energy after insertion), or else the excess chemical potential energy of the system. One insertion-attempt involves first keeping all other particles in the domain frozen in space and time. A new "trial" molecule is then inserted randomly in the MD domain, and is shifted away from the overlapping core of resident molecules in an iterative manner, guided by the strength and slope of the static potential energy landscape. At each prospective shift, the sum of pair-forces of the trial molecule with all neighbouring molecules within the cut-off range is computed. The direction of the force is used for the next translation shift in the iteration. For water molecule insertions,[24] the steepest-descent scheme includes rotational updates in addition to translational shifts. Unsuccessful shifting terminates when the algorithm detects a trap in the energy landscape, which is measured by a repetitive downhill-uphill variation of energy, or when too many attempts are performed that makes it worthwhile to stop the site-searching and wait until a later time in the simulation.

The main disadvantages of the USHER algorithm are that it requires the correct selection and optimisation of the input parameters to minimise computational cost and maximise insertion rate. It is a serial method, so multiple insertions within a region of the domain smaller than the potential cut-off need to be done in succession, as every insertion influences the local energy landscape. As a result, this precludes a reasonable parallel implementation of the algorithm. Finally, the USHER method has so far been developed for relatively small atoms/molecules (Lennard-Jones atoms and TIP3P water molecules), but it is yet to be shown whether it is applicable to inserting larger molecules (e.g., polymers) and macro molecules (e.g., fullerenes) that are typically situated at much lower potential energies (i.e., harder to find sites) than those of monatomic and water solvents.

In this paper we propose a new mass-statting method called FADE, which offers an alternative insertion protocol to USHER and also incorporates a deletion protocol (symmetrical and in reverse to insertion) for use within the MD and hybrid-MD simulation community. It is simple, has low computational expense, has negligible effect on the overall system dynamics, and high insertion rates are achievable. Unlike USHER, FADE enables the insertion of a wider variety of molecules, ranging from atoms to large macromolecules, and can be done in parallel.

The premise of the FADE algorithm (as the name suggests) is to apply gradual adjustments to the van der Waals and electrostatic pair intermolecular forces for the inserting (FADE-in) or deleting (FADE-out) molecule, applied through a relaxation coefficient that is weighted by time. The "fading" process is artificial but it inherently conserves overall system momentum, since the weighting is applied between pairs of molecules. The choice of weighting function is important, and dependent on the fluid state and size of the inserting molecule, but can be described using only two parameters: the relaxation time-scale, and the order of the polynomial. We also propose an optimisation scheme for choosing initial sites when inserting smaller molecules such as monatomics and water. It consists of computing the minimum separation between existing molecules and using this as a basis for placing inserting molecules away from existing ones, and hence at a lower and more favourable energy. This makes FADE extremely stable and enables shorter relaxation insertion times.

The rest of this paper is organised as follows. In Sec. II we describe how mass-statting can be performed using the FADE method in MD simulations, while in Sec. III various verification examples for different molecules are presented in simple configurations. Finally in Sec. IV we conclude, and discuss mass-statting for future applications.

II. METHOD

A. Molecular dynamics

All molecules in a general molecular dynamics simulation evolve in time t and space $\mathbf{r} = (x, y, z)$ according to Newton's equations of motion:

$$\frac{d\mathbf{r}_i}{dt} = \mathbf{v}_i, \quad \text{and} \quad m_i \frac{d\mathbf{v}_i}{dt} = \mathbf{f}_i, \tag{1}$$

where $i = (1, 2, \ldots, N)$ is the index of a molecule in a system of N molecules, and $m_i, \mathbf{r}_i, \mathbf{v}_i, \mathbf{f}_i$ are the molecule's mass, position, velocity, and total force, respectively. The total force on a molecule (which also includes thermostatting forces) is computed from a sum of pair intermolecular forces with neighbouring molecules by

$$\mathbf{f}_i = \sum_{j=1(\neq i)}^{N} -\nabla U(r_{ij}), \tag{2}$$

where $U(r_{ij})$ is the pair-wise potential and $r_{ij} = |\mathbf{r}_i - \mathbf{r}_j|$ is the separation of two arbitrary molecules (i, j). Equation (1) are integrated numerically—which in this paper consists of the Verlet algorithm—using a discrete time step Δt, while the pair force calculation step in Eq. (2) is computationally optimised by using double-loop savings, a cut-off distance r_{cut}, and the cell-list algorithm.[25] Our MD code is implemented

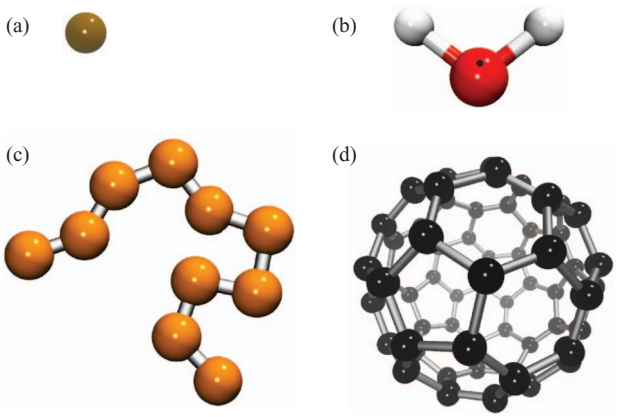

FIG. 1. The molecules considered for insertion and deletion using the FADE algorithm: (a) argon atom, (b) rigid TIP4P/2005 water model, (c) flexible 10-bead polymer strand using FENE model, (d) rigid "buckyball" C_{60} molecule.

in the OpenFOAM software libraries,[26] and has been used to study various nano-/micro-scale fluid dynamics problems, e.g., Refs. 5 and 13 and 27–30.

In this paper we demonstrate the simulation capabilities of the FADE algorithm by showing insertion and deletion of various atoms, molecules, and macro molecules. Four types of atomistic/molecular systems are considered, as illustrated in Figure 1; the models are described individually in Sec. III.

B. Mass-statting

A mass-stat is analogous to a thermostat[31,32] or a velocity/momentum constraint.[4,33,34] In the former, the equations of motions of the particles are modified by connecting them to a fictitious heat bath at a given temperature, for example, by rescaling molecular velocities[32] or by applying thermalising forces.[35,36] In the latter, velocities of molecules are rescaled to match a target momentum or streaming velocity. The strength of the coupling in any thermostatting or momentum-statting procedure is in most cases dependent on a pre-specified timescale that typically consists of $\mathcal{O}(10)$ to $\mathcal{O}(100)$ MD time steps, and which is determined *a priori* from MD simulations. In most cases, this timescale has to be carefully chosen as it could either impact important thermal fluctuations or introduce chances of blow-up if selected too small. If the time coupling is chosen too large, a time-lag for obtaining a target temperature/momentum might be introduced (which is undesirable in unsteady problems) or even an inadequate coupling.

The mass-stat we propose in this paper follows the same methodology as thermostats and momentum-stats. In particular, it adopts a time-scale τ_T for the gradual insertion or deletion of molecules at prescribed spatial and temporal points of a molecular dynamics simulation. Alike to every statting procedure, the parameters of the mass-stat also should be carefully chosen so as not to introduce spurious changes to the potential energy U and kinetic energy of the system, and to avoid simulation blow-up.

FADE fits well within these mass-statting requirements. In FADE, insertion and deletion processes are dealt with separately, which we term FADE-in and FADE-out, respectively, and are symmetric to one another, as we explain shortly. To prevent energy changes in the system, FADE adopts a relaxation scheme applied during the intermolecular force computation step for the van der Waals and electrostatic forces only; FADE-ing of strong intra-molecular bonds is generally not necessary.

To explain the relaxation procedure of FADE, let us assign every molecule in the system a weighting coefficient, $\omega_i = 1$, unless it is being inserted/deleted, in which case it has a time-varying weight $\omega_i(t) \in [0, 1]$, $t \in [0, \tau_T]$. The intermolecular force between any pair of interacting atoms (say i and j), given by $f_{ij}(r_{ij}) = -\nabla U(r_{ij})$ in Eq. (2), is now modified to include the combination of coefficients, $\omega_{ij} = \min(\omega_i, \omega_j)$ such that

$$f_{ij}(r_{ij}) = \begin{cases} -\omega_{ij}\nabla U(r_0) & \text{if } 0 \le r_{ij} < r_0, \\ -\omega_{ij}\nabla U(r_{ij}) & \text{if } r_0 \le r_{ij} < r_{\text{cut}}, \\ 0 & \text{if } r_{ij} \ge r_{\text{cut}}, \end{cases} \tag{3}$$

where r_0 is a minimum distance below which the potential becomes unrealistically large and unattainable during a normal simulation. This truncates the potential and prevents the computation of extremely large numbers should the separation of two molecules approach zero during any given FADE operation.

For FADE-in, a new molecule i is inserted with $\omega_i = 0$ and its relaxation coefficient is gradually increased to 1 through the following time-dependent weighting function:

$$\omega_i(t) = \begin{cases} (2t/\tau_T)^n/2 & \text{if } \quad t < \tau_T/2, \\ 1 - |(2[t - \tau_T]/\tau_T)^n|/2 & \text{if } \quad \tau_T/2 \le t < \tau_T, \\ 1 & \text{if } \quad t \ge \tau_T, \end{cases} \tag{4}$$

where τ_T is the insertion time-scale (through which ω_i: $0 \to 1$), $t = 0, \Delta t, 2\Delta t, \ldots, \tau_T$ is the reference time from the moment of insertion and n is the order of the piecewise polynomial that defines the time-variation of the weighting. A larger value of n makes the time longer for which the weighting is close to zero, and so enables a more gradual weighting to begin with. On the other hand, an excessively large value for n, while not only not being necessary is also undesirable because it makes the weighted function approach the Heaviside form, which eliminates the essential time-relaxation feature. We propose appropriate choices for n and τ_T in Sec. III. The initial velocity of the inserted molecule is randomly selected from a Maxwell-Boltzmann distribution at the target velocity and temperature, which is consistent with other work.[23]

For FADE-out, an existing molecule is first *highlighted* for deletion (it is not yet removed from the MD domain), followed by a transition period that is the reverse of the FADE-in process, i.e., the relaxation coefficient is gradually reduced to zero (ω_i: $1 \to 0$). The time-varying weighting function for deletion is therefore

$$\omega_i(t) = \begin{cases} 1 - (2t/\tau_T)^n/2 & \text{if } \quad t < \tau_T/2, \\ |(2[t - \tau_T]/\tau_T)^n|/2 & \text{if } \quad \tau_T/2 \le t < \tau_T/2, \\ 0 & \text{if } \quad t \ge \tau_T. \end{cases} \tag{5}$$

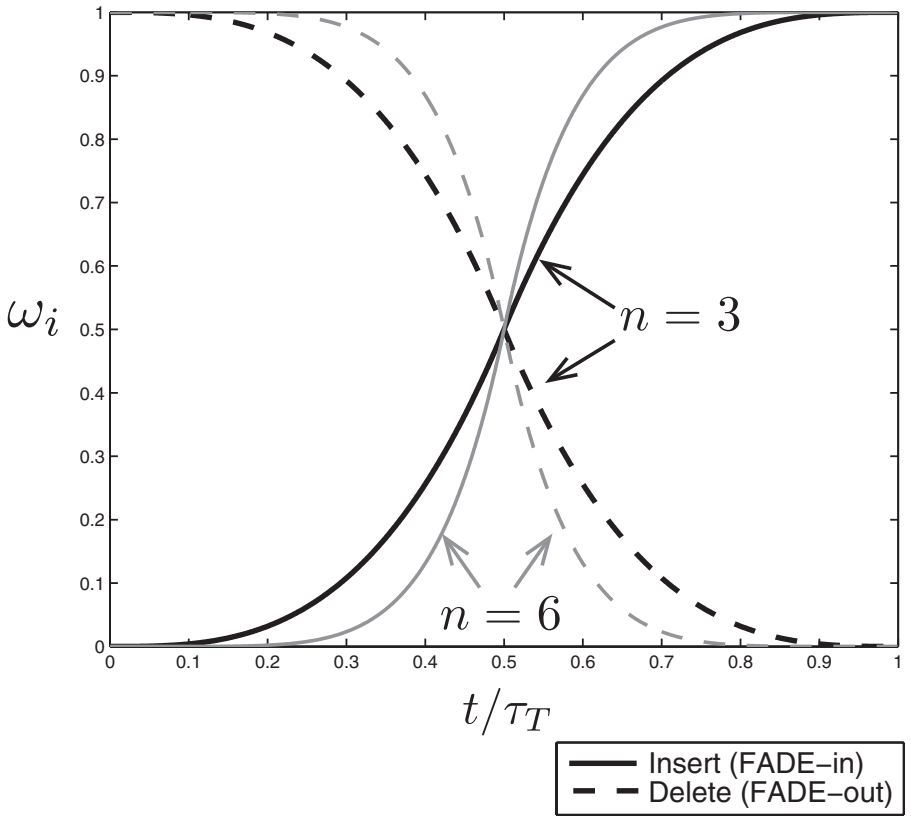

FIG. 2. Weighting functions ω_i varying with normalised time units applied to the intermolecular force calculation for those molecules going through a FADE-in (—) or FADE-out (- - -) process. Taken from Eqs. (4) and (5) with polynomial degrees $n = 3$ and $n = 6$ as indicated.

When ω_i becomes zero (after the transition time τ_T), the molecule can be removed from the system without any problem. The variation of the weighting functions for insertion and deletion, Eqs. (4) and (5), respectively, are shown in Figure 2, for $n = 3$ and $n = 6$.

Equation (3) has been constructed to inherently obey Newton's third law ($f_{ij} = -f_{ji}$), no matter the choice of weighting function $\omega_i(t)$ for FADE-in or FADE-out. Therefore, conservation of overall momentum is always guaranteed in our method. This momentum-conserving attribute is also seen in thermostats for dissipative particle dynamics (DPD),[35,37] in which random and dissipative pair-wise opposite forces are added to molecules to control local temperature. While these thermostats normally also conserve mass and total system energy, in our case, however, we are modelling the physics of a mass-stat so mass can never be conserved, and neither can total energy. The latter property has been demonstrated in detail in Ref. 23. In the present paper we assume isothermal conditions, and a thermostat needs to be applied in conjunction with the mass-stat; any changes of mass will then contribute directly to virial (pressure) changes.

What we have yet to discuss is the choice of initial site at which a molecule is inserted for the FADE-in method. This choice can be made without prior knowledge of the positions of the existing molecules. We call this method the Pure-FADE approach, and is applicable to all the molecules illustrated in Fig. 1. Molecules can be distributed randomly or, preferably, uniformly within the domain at every given insertion instance. Uniform distribution of molecules is preferred because the effect on the dynamics of the surrounding fluid is minimised when molecules are reasonably spaced out during tandem insertion. Pure-FADE simulations will not blow up provided the correct choice for n and τ_T are made, as we demonstrate in Sec. III.

For small molecules, such as water and monatomic argon, the choice of initial site for an inserting molecule can however be improved. Although the initial force is zero on a newly-inserted molecule i (because initially $\omega_i = 0$), it is best if the initial site is chosen to be as far away as possible from all other molecules. We found that this additional step enables us to choose a smaller value of n and, more importantly, a shorter insertion time scale τ_T. We call this addition to the FADE algorithm, the Optimal-FADE approach. Its benefits include minimising spurious heat entering into the system, which in turn avoids any expensive thermalisation steps. It eliminates simulation blow-up and also enables a very high insertion rate even in reasonably dense liquids. We demonstrate these characteristics in Sec. III.

We calculate the maximum amount of "clearance" available around existing molecules and term this the *minimum separation* property. It essentially describes the instantaneous structural configuration of the fluid (such as the radial distribution function). Consider an existing molecule j ($\neq i$), with i being the molecule to be inserted. The minimum separation of j, denoted by $\tilde{r}_j$, from all other existing neighbouring molecules k ($\neq i, \neq j$) is found as the minimum of all pair spatial separations r_{jk}, i.e., $\min(r_{jk})$.[38] The initial site of i is then picked anywhere on the surface of an imaginary sphere

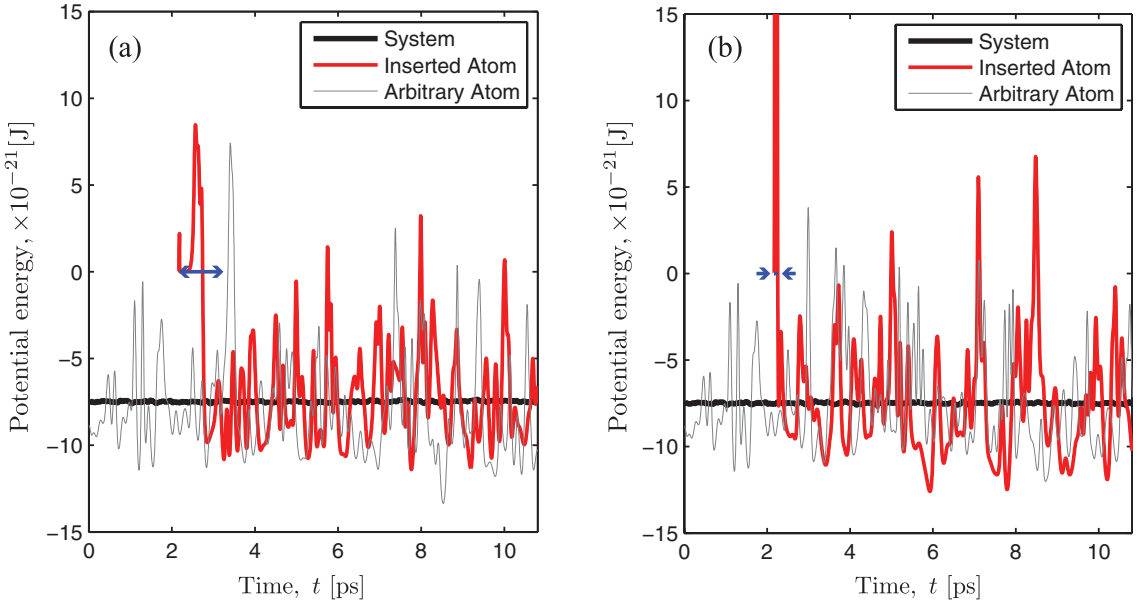

FIG. 3. Potential energy measurements during the insertion of one atom within a periodic cube of dense liquid argon ($\rho = 1566$ kg/m^3, $N = 3768$ atoms, $T = 293$ K) using (a) the Pure-FADE approach, $n = 10$, $\tau_T = 200\Delta t$, and (b) the Optimal-FADE approach $n = 3$, $\tau_T = 20\Delta t$. In each figure we present the mean system energy (black solid line), the energy of the inserted molecule (red line), and the energy of an arbitrary existing atom (gray line) for comparison of fluctuations. The horizontal blue arrow indicates the insertion time τ_T. In all cases the system potential energy remains unaffected by insertion. The insertion variation for this case is $\Delta N/N = 1/3768 \approx 0.03\%$.

of radius $\tilde{r}_j/2$, centred at the chosen molecule $\mathbf{r}_j$, given by $\mathbf{r}_i = \mathbf{r}_j + \vec{\xi}\,\tilde{r}_j/2$, where $\vec{\xi}$ is a random unit vector.

III. RESULTS AND DISCUSSION

A. Argon

MD simulations of the insertion of one argon atom within a domain are first shown using both the Optimal-FADE and the Pure-FADE techniques, for different FADE parameters n and τ_T. A periodic cube of side-length 5.44 nm is initially filled with highly dense liquid argon: $\rho = 1566$ kg/m^3, $N = 3768$ atoms, at temperature $T = 293$ K. The atoms are described by the 12-6 Lennard–Jones (LJ) potential (see Fig. 1(a)):

$$U_{LJ}(r_{ij}) = 4\epsilon\left[\left(\frac{\sigma}{r_{ij}}\right)^{12} - \left(\frac{\sigma}{r_{ij}}\right)^{6}\right], \qquad (6)$$

where ϵ and σ are the potential's characteristic energy and length scales; for argon these are $\epsilon_{Ar-Ar} = 0.9977$ kJ mol^{-1} and $\sigma_{Ar-Ar} = 3.4$ Å. In every simulation for argon presented in this section, the MD time step is fixed at $\Delta t = 5.4$ fs, and the cut-off radius, $r_{\text{cut}} = 1.36$ nm. The insertion site in the Pure-FADE approach is chosen to be the worst-case site, i.e., when the new atom is placed exactly overlapping another atom. Although this occurrence is infrequent, in principle it is still possible and so we use this worst-case scenario to assess the insertion parameters n and τ_T that produce a stable outcome. In all cases in this section we apply also a Berendsen thermostat[32] with a fixed time constant of $4\Delta t$.

In Figure 3 we present potential energy measurements taken at every time step from the Pure-FADE and Optimal-FADE simulations, respectively, for selected parameters n and τ_T. We see that in all cases the energy of the system is unaffected during insertion of the atom, and that the potential energy of the inserted molecule behaves like that of an existing atom in the system after it has fully been inserted (i.e., after time τ_T has passed). Figure 4 gives a tabulated overview of all the cases considered for n and τ_T. Simulations which blew up are indicated by the "×" symbol. In terms of robustness, we found that the Optimal-FADE is stable for all values of n and τ_T considered. The Pure-FADE approach on the other hand is less robust, as indicated in Figure 4(a), so care must be taken when choosing these parameters. In this exercise, values of $n = 10$ and $\tau_T = 400\Delta t$ are sufficient to prevent blow-up if Pure-FADE is used.

n \ $\tau_T/\Delta t$	40	200	400	800	4000
5	×	×	×	×	×
6	×	×	×	×	
7	×	×	×	×	
8	×	×			
9	×	×			
10	×				

(a)

n \ $\tau_T/\Delta t$	20	40	200	400	800
2					
3					
4					
5					
6					
7					

(b)

FIG. 4. Overview of the robustness characteristics of the (a) Pure-FADE and (b) Optimal-FADE techniques for the insertion of one atom in highly dense argon liquid, for various insertion parameters n and τ_T. The symbol "×" indicates simulation blow-up for that particular combination of parameters. It is clear that the Optimal-FADE is more robust than the Pure-FADE approach, and also allows for shorter insertion times.

Deletion of one atom for this test case has also been carried out for decreasing values of τ_T, but we found deletion to affect the molecules' dynamics less than insertion. The effect of FADE-out becomes more important when multiple molecules need to be deleted, or when the deleted molecule strongly interacts with its local environment, such as the long range Coulomb forces in water (Sec. III B), and entangled long polymer strands (Sec. III C).

The next test demonstrates the ability of the FADE algorithm to efficiently insert numerous molecules at any given instance, without simulation blow-up. There are two scopes for this test. First, in common setup procedures where a *pre*-MD simulation is used to drive the system towards an initial (accurate) target thermodynamic state, the ability to insert a large number of molecules in a short period of time[39] is essential to reduce the computational cost of this pre-simulation. Most importantly, however, whenever insertion is required in a steady or time-accurate MD simulation (e.g., to apply thermodynamic or hydrodynamic constraints), these test simulations are useful for choosing the insertion parameters n and τ_T, as well as the highest insertion variation ratio $\Delta N/N_0$, to reduce spurious, unwanted spikes in the system energy to within an acceptable level. Here, ΔN is the number of instantaneously inserted atoms, and N_0 is the number of existing atoms prior to insertion.

The Optimal-FADE method is now used on the same periodic case as before ($\rho_0 = 1566$ kg/m^3, $N_0 = 3768$ atoms) to insert at a given instance the following number of argon atoms distributed evenly across the domain: $\Delta N = 1$, 30, 60, 100, and 1000. These correspond to quasi-instantaneous density variations ($\Delta N/N_0$) of 0.03%, 0.8%, 1.6%, 2.7%, and 26.5%, respectively. The potential energy measurements for the two largest insertion cases, $\Delta N = 100$ and $\Delta N = 1000$, are displayed in Figures 5 and 6, respectively. We see that the system energy in these cases is influenced severely by the large insertions, as shown by the spikes in the system energy (black solid line) during the insertion time (blue horizontal arrow). Evidently, the number of atoms inserted within a fixed time scale τ_T (a numerical control parameter) exceeds a physical rate at which these molecules should be inserted. Despite blow-up not occurring, these tests can help to determine the correct choice of parameters that minimises the energy introduced during an insertion, prior to use in full MD simulations. Therefore, we highlight in Figure 7 the magnitude of the potential energy spike in the system ΔU (i.e., the excess energy caused by insertion), in relation to the target potential energy U_t (i.e., the equilibrium energy after insertion) in all these simulations. We choose a 5% energy excess as the maximum allowable, in accordance with the threshold value chosen in the USHER algorithm.[23] As a result, a recommended choice of insertion time and insertion variation at any instance when using the Optimal-FADE method for argon is $\tau_T/\Delta t \geq 200$ and $\Delta N/N_0 < 3\%$–4%, respectively. For problems where shorter relaxation times (τ_T) are necessary, the molecule insertion rate needs to be lowered substantially, in accordance with Figure 7.

In the last test case we apply the Optimal-FADE algorithm within an automated MD simulation to generate pressure-density curves at a fixed temperature for argon. This demonstrates FADE operating over a large range of densities within one simulation. The periodic cube is now set to a larger side length of 10.88 nm to improve statistics when measuring pressure, and starts off at an initial low density ($\rho_0 = 340$ kg/m^3, $N_0 = 6554$ atoms). At every density increment, $\Delta N = 246$ argon atoms are inserted instantaneously with parameters $n = 3$ and $\tau_T = 400\Delta t$. This corresponds to an instantaneous variation of density of 3.7% at the lowest density, up to 0.8% at the highest density, which satisfies the condition to keep any energy changes below 5%. The Berendsen thermostat with a time-constant of $4\Delta t$ is applied during the insertion period. After insertion, a time of $800\Delta t$ is then allocated to measure density and pressure accurately in the

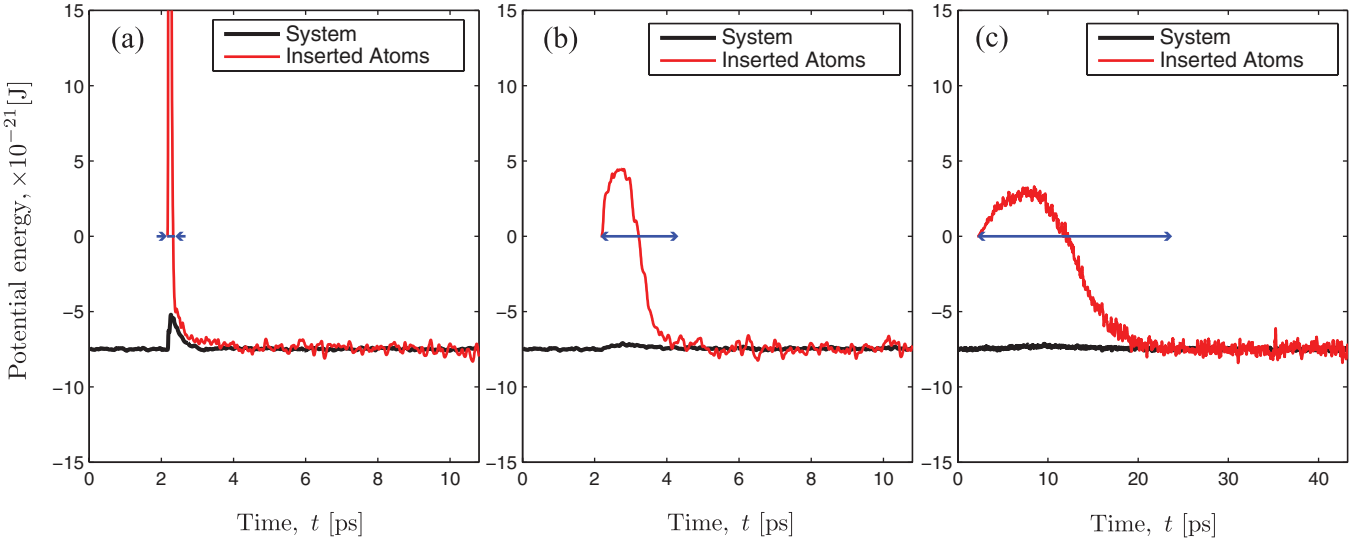

FIG. 5. Potential energy measurements during the insertion of 100 atoms within a periodic cube of dense liquid argon ($\rho_0 = 1566$ kg/m^3, $N_0 = 3768$ atoms, $T = 293$ K) using the Optimal-FADE approach (fixed $n = 3$): (a) $\tau_T = 40\Delta t$, (b) $\tau_T = 400\Delta t$, and (c) $\tau_T = 4000\Delta t$. In each figure we present the mean system energy (black solid line) and the mean energy of the inserted atoms (red line). The horizontal blue arrow indicates the insertion time τ_T. The insertion variation for this case is $\Delta N/N_0 = 100/3768 = 2.7\%$.

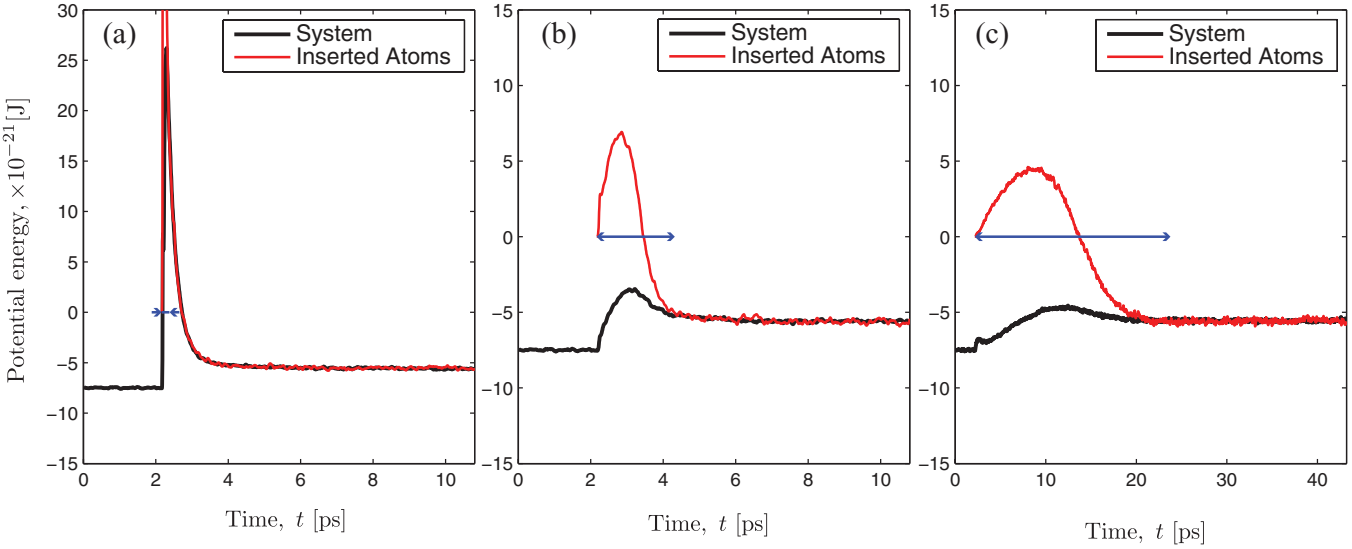

FIG. 6. Potential energy measurements during the insertion of 1000 atoms within a periodic cube of dense liquid argon ($\rho_0 = 1566$ kg/m^3, $N_0 = 3768$ atoms, $T = 293$ K) using the Optimal-FADE approach (fixed $n = 3$): (a) $\tau_T = 40\Delta t$, (b) $\tau_T = 400\Delta t$, and (c) $\tau_T = 4000\Delta t$. In each figure we present the mean system energy (black solid line) and the mean energy of the inserted atoms (red line). The horizontal blue arrow indicates the insertion time τ_T. The insertion variation for this case is $\Delta N/N_0 = 1000/3768 = 26.5\%$.

domain, during which no control is applied. This is repeated 100 times, to generate a table of pressure values between $\rho = 340$ kg/m^3 and $\rho = 1617$ kg/m^3. The pressure-density plots for three separate temperatures ($T = 292.8$ K, $T = 216$ K, and $T = 84$ K) are displayed in Figure 8, which also compares our results to the same simulations using the USHER algorithm,[23] and independent MD results of Johnson *et al.*[40] Clearly, all three results agree exceptionally well.

The simulations for USHER and FADE in this latter exercise were all performed in serial on the same machine to enable a fair comparison of computational cost. In Figure 9(a) we present processor clock data for the duration of the insertion slot ($400\Delta t$) at each increment. While Optimal-FADE is computationally as efficient as USHER at low fluid densities, our simulations show that FADE offers a better performance at higher densities. Figure 9(b) shows the computational cost for the lowest temperature, where we also see the major computational savings afforded by running FADE on 8 processor cores. A parallel implementation of the USHER algorithm is much more involved, as mentioned in the introduction of this paper, and so has been omitted from this analysis. The problem with USHER is that it is inherently a serial process—the potential energy landscape must be frozen during every insertion. Tandem insertions are only possible if the insertion site (which is not known *a priori*) of every new molecule is selected at least a cut-off radius r_{cut} away from other molecules being inserted. In a parallel-processing simulation (for example where the MD domain is decomposed on several

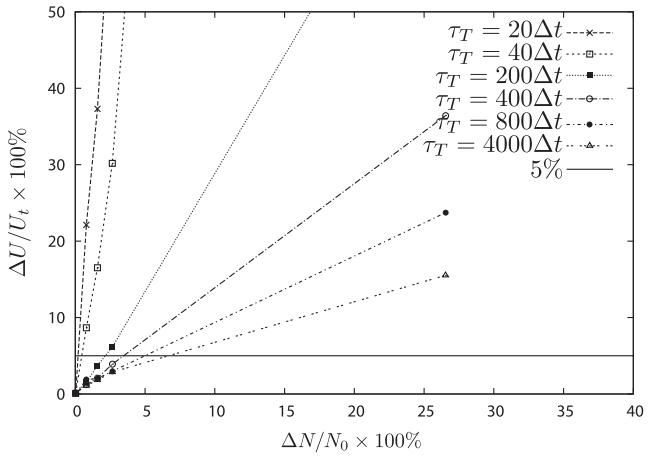

FIG. 7. Percentage change in system potential energy during insertion of argon atoms, against insertion ratio, for various relaxation times τ_T at fixed $n = 3$ using the Optimal-FADE approach. We recommend running MD cases that stay below the horizontal solid line (5%).

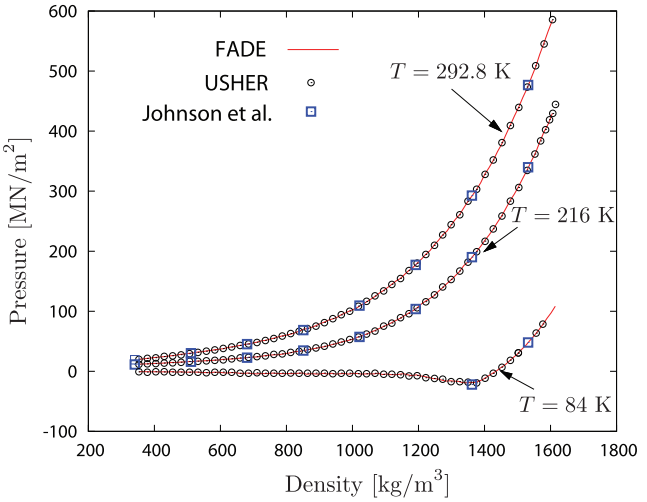

FIG. 8. Isothermal pressure-density curves generated for argon using FADE (—) and USHER (○) insertion algorithms at fixed temperatures: $T = 292.8$ K, $T = 216$ K, and $T = 84$ K. Parameters for FADE are $n = 3$, and $\tau_T = 400\Delta t$, while USHER parameters are taken from Ref. 23. MD results for the same Lennard-Jones fluid taken from Johnson *et al.*[40] are also plotted for reference (□).

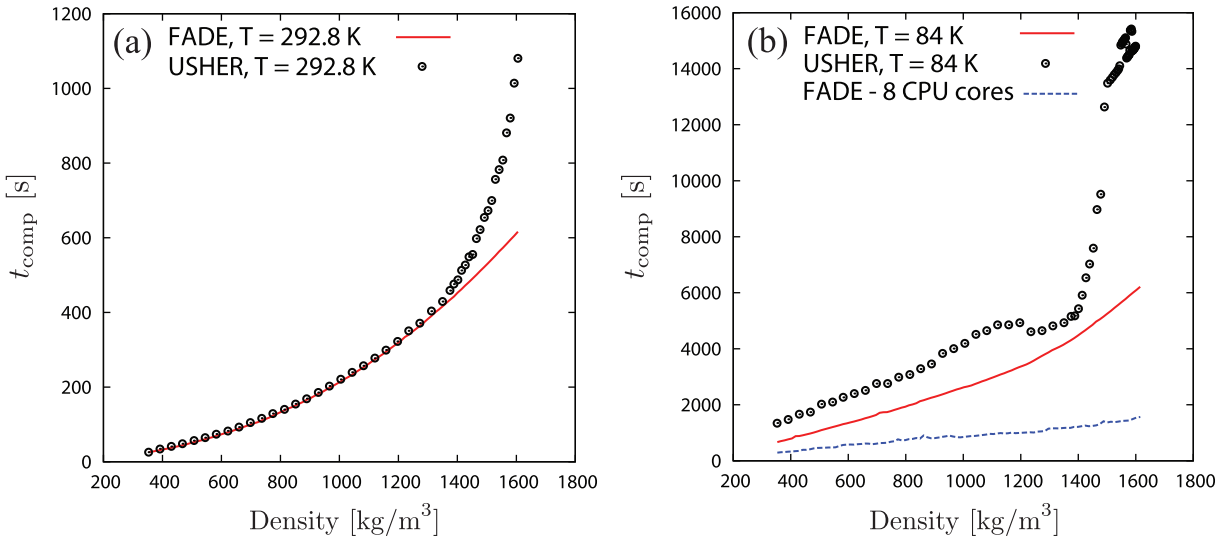

FIG. 9. Computational cost comparisons on a single processor between USHER (○) and FADE (—) algorithms for the pressure-density simulations of argon at (a) $T = 292.8$ K and (b) $T = 84$ K. The cost is taken as the processing time t_{comp} of the MD simulation for an allocated period, (a) $400\Delta t$ and (b) $4000\Delta t$, respectively, during which insertion and thermostatting both occur simultaneously. In (b) we also see the computational savings when running the FADE simulation on eight processors, instead of one. No parallel USHER results are presented because the parallel implementation for this algorithm is more complicated.

processors[41]), we believe a general USHER implementation would require that all molecules be inserted in serial.

B. Water

We now repeat the same test cases in Sec. III A but instead with the rigid TIP4P/2005 water model for condensed phases of water.[42–44] The water model is illustrated in Figure 1(b), and consists of four interacting sites: one oxygen atom (O) with no charge but which is the centre of the Lennard-Jones potential, two hydrogen sites (H) each with a fixed point charge of $q_H = 0.5564\ e$, and a massless site (M) with charge $q_M = -1.1128\ e$. All oxygen atoms interact using the Lennard-Jones potential, Eq. (6) with $\epsilon_{O-O} = 0.7749$ kJ mol^{-1} and $\sigma_{O-O} = 3.1589$ Å, while the other charged sites interact via the Coulomb potential:

$$U_C(r_{ij}) = \frac{1}{4\pi\epsilon_0}\frac{q_i q_j}{r_{ij}}, \tag{7}$$

where q_i, q_j are the site charges and ϵ_0 is the vacuum permittivity. The time step for all water simulations is set to $\Delta t = 2.16$ fs, and the cut-off radius is set to $r_{\text{cut}} = 1.0$ nm for all interactions.

A periodic cube of side length 6.12 nm is initialised with high pressure water at $p = 200$ MPa, $N = 8216$ molecules, and $T = 283$ K, making this a suitably dense case for demonstrating the FADE method. Controlling water at high pressure is important in our work on pressure-driven flows through nanotube membranes.[13,29] One water molecule is inserted

		$\tau_T/\Delta t$				
		100	500	1000	2000	10000
n	5	×	×	×	×	
	6	×	×			
	7	×	×			
	8	×				
	9	×				
	10					

FIG. 10. Overview of the robustness characteristics of the Pure-FADE approach for the insertion of one water molecule in high pressure water, for various insertion parameters n and τ_T. The symbol "×" indicates simulation blow-up for that particular combination of parameters.

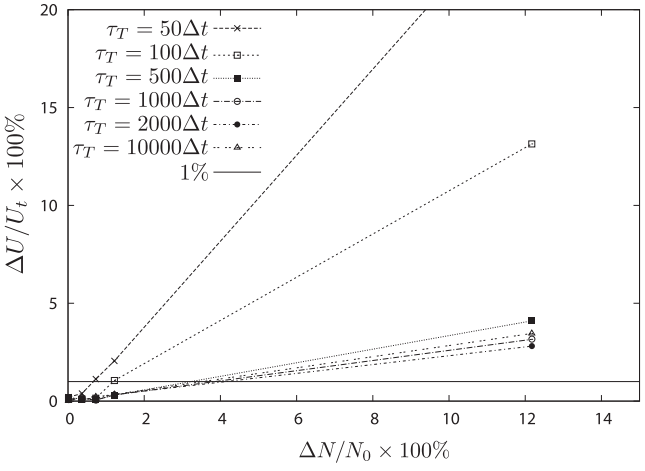

FIG. 11. Percentage change in system potential energy during insertion of water molecules using Optimal-FADE, against insertion ratio, for various relaxation times τ_T at fixed $n = 3$. In full MD simulations, where energy minimisation is important, we recommend running cases that stay below the horizontal solid line (1%).

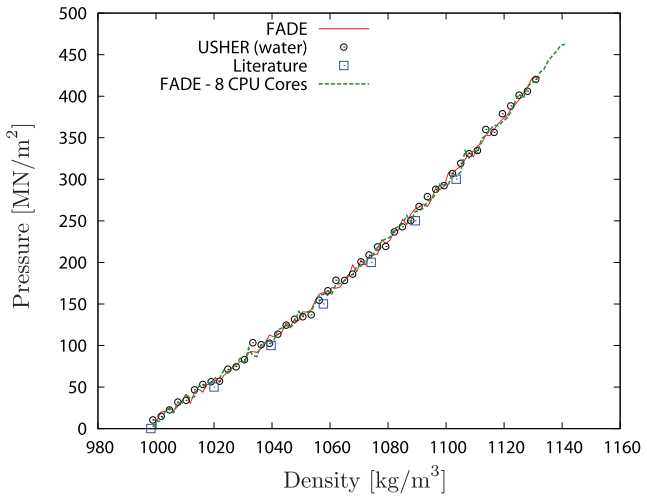

FIG. 12. Isothermal pressure-density curves generated for water using both FADE and USHER insertion algorithms at a fixed temperature $T = 292.8$ K. Parameters for FADE are $n = 4$, and $\tau_T = 1000\Delta t$, while USHER parameters are taken from Ref. 47. Pressure-density results from Ref. 46 are also plotted.

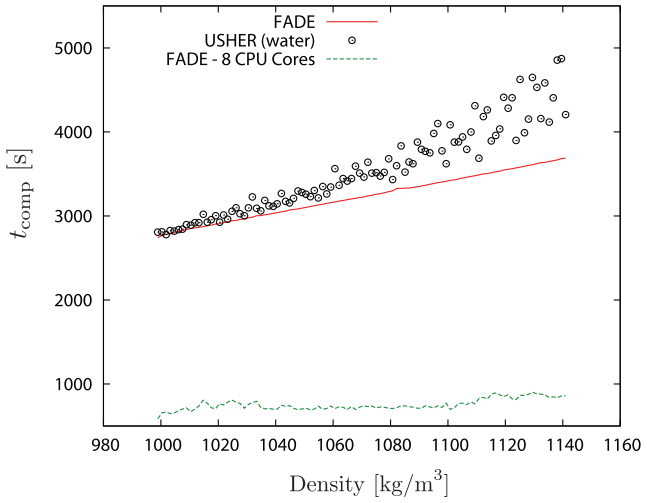

FIG. 13. Computational cost comparisons between FADE (both serial and parallel) and USHER algorithms for the pressure-density simulations of water at $T = 292.8$ K. The cost is taken as the processing time t_{comp} of the MD simulation for an allocated period ($2000\Delta t$) during which insertion and thermostatting both occur simultaneously. The efficiency of the parallel implementation of FADE can clearly be seen.

using the Optimal-FADE and Pure-FADE approaches exactly as before. The Optimal-FADE showed no instabilities for the range of insertion parameters n and τ_T considered (similar to the simulations for argon), while the Pure-FADE showed simulation blow-up, as presented in Figure 10.

Multiple water insertion tests are also carried out as before to determine *a priori* the insertion parameters that restrict energy changes to within an acceptable range. In this case we use smaller percentage variations of inserted molecules: 0.01%, 0.4%, 0.7%, 1.2%, and 12.1%. Figure 11 shows the overall results, with the recommendation to select density variation and time-relaxation parameters that keep potential energy changes below 1%.[45] This means $\Delta N/N_0 < 3\%$–4% and $\tau_T/\Delta t \geq 500$, respectively.

Finally we generate a density-pressure curve at room temperature to show the behaviour of water from atmospheric conditions up to very high pressures. In Figure 12 we compare the results of the Optimal-FADE algorithm with those of a water-USHER implementation, and data taken from the NIST database for water.[46] From Figure 13 we can again deduce that FADE is at least as computationally efficient as USHER.

C. Pseudoplastic polymer melts

We now demonstrate the capabilities of the FADE algorithm where the USHER algorithm is no longer valid; that is, for insertion and deletion of larger molecules. In this case we apply FADE-in and FADE-out to high aspect ratio polymers in polymer melts of varying strand-density. The model for a pseudoplastic polymer fluid we consider here consists of molecular strands, with 10 connected beads (atoms) per strand,[28,48] see Figure 1(c). Every bead in the strand is connected to its neighbour via a finitely extensible nonlinear elastic (FENE) potential:

$$U_{\text{FENE}}(r_{ij}) = \begin{cases} -0.5kr_1^2 \ln\left[1 - \left(\frac{r_{ij}}{r_1}\right)^2\right] & \text{if } r_{ij} < r_1, \\ \infty & \text{if } r_{ij} \geq r_1, \end{cases} \tag{8}$$

where $k = 0.43$ kg s^{-2} is the FENE spring constant and $r_1 = 5.1$ Å is the finite extensibility of a pair of connected

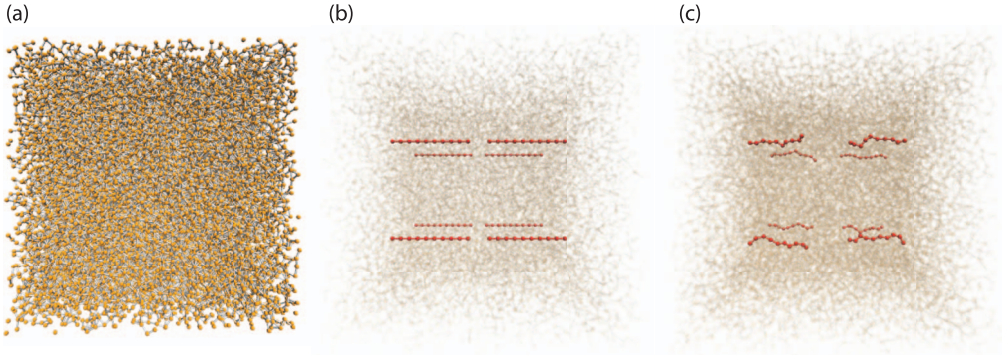

FIG. 14. Snapshots from the MD simulation: (a) polymeric melt at a bead density $\rho = 1407$ kg/m^3, (b) uniform placement of 8 polymer strands, and (c) complete insertion of polymers after FADE-in with parameters $\tau_T = 2000\Delta t$ and $n = 10$.

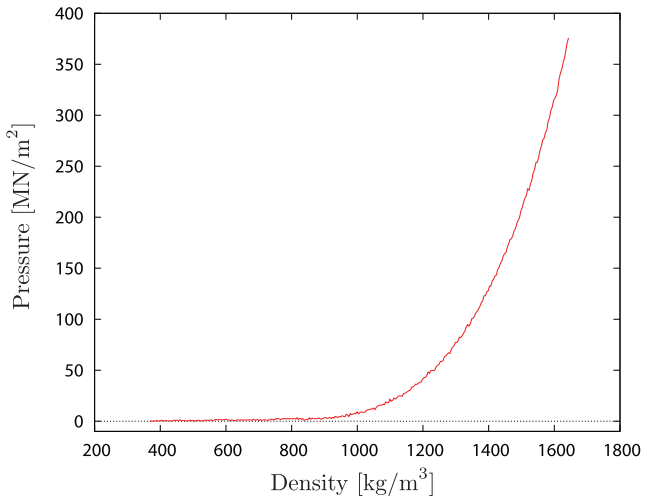

FIG. 15. Isothermal pressure-density curve generated at constant $T = 292.8$ K for a 10-bead-strand polymeric fluid. Note, mass density on the x-axis is based on bead density, not strand density.

beads. These properties are chosen from Refs. 49 and 50 in order to minimise bond cross-overs. A LJ potential (6) is also applied between all beads within the cut-off distance, with the same parameters as argon. As described in Sec. II B, during insertion only the LJ intermolecular potential undergoes FADE-in; the intramolecular FENE bond is not affected by the FADE operation.

We generate, as before, a pressure-density curve at constant temperature within a periodic cube of side length 10.9 nm, which is chosen large enough so that an extended polymer (~4.6 nm) does not interact with itself across the periodic boundaries. Pure-FADE is used for strand insertion, where the choice of insertion parameters is taken from the analysis of argon in Sec. III A, i.e., $n = 10$, $\tau_T = 2000\Delta t$, where $\Delta t = 2.16$ fs. Eight strands are inserted at every time-increment ($7000\Delta t$) uniformly within the domain, the first $\tau_T = 2000\Delta t$ is the insertion time, the next $3000\Delta t$ is allowed for polymeric relaxation, and finally a time interval of $2000\Delta t$ is for measuring pressure and density. Figure 14 demonstrates insertions of these polymers at a high melt density $\rho = 1407$ kg/m^3. During insertion, the Andersen stochastic thermostat is applied with a probability of heat bath collisions of 0.02.[31] The pressure-density curve is presented in Figure 15. Note that we repeated this polymeric simulation with increasing values of relaxation time and in reverse, i.e. where FADE-out is used to delete strands gradually from the melt. In every case, no deviation from the pressure-density curve presented in Figure 15 was observed.

D. Buckminsterfullerene, C_{60}

Finally, we demonstrate the versatility of the FADE algorithm by applying simultaneous FADE-in and FADE-out operations to deal with hollow macro molecules. We simulate the insertion and deletion of C_{60} Buckminsterfullerene molecules—which we hereon refer to as "buckyballs"—within an argon solvent. The buckyball is a spherical macromolecule of radius $R = 3.5$ Å composed of 60 carbon atoms modelled explicitly and linked by hexagonal rings, as shown in Fig. 1(d). The buckyball is modelled as a rigid polyatomic molecule with six degrees of freedom and no intramolecular degrees of freedom. Between different buckyballs and the solvent fluid, van der Waals forces are modelled using the LJ potential with parameters $\epsilon_{C-C} = 0.4396$ kJ mol^{-1} and $\sigma_{C-C} = 3.851$ Å for carbon-carbon interactions taken from Ref. 51, and $\epsilon_{C-Ar} = 0.6623$ kJ mol^{-1} and $\sigma_{C-Ar} = 3.626$ Å for carbon-argon interactions. The latter set of parameters are obtained using the Lorentz-Berthelot mixing rules.[1]

As the buckyballs are hollow, we found in our insertion simulations that a FADE approach almost always traps a few solvent atoms within it, which puts the buckyball at a very high (unrealistic) total energy. We solve this by immediately *highlighting* the trapped solvent atoms for FADE-out as soon as a buckyball is inserted, and then *simultaneously*

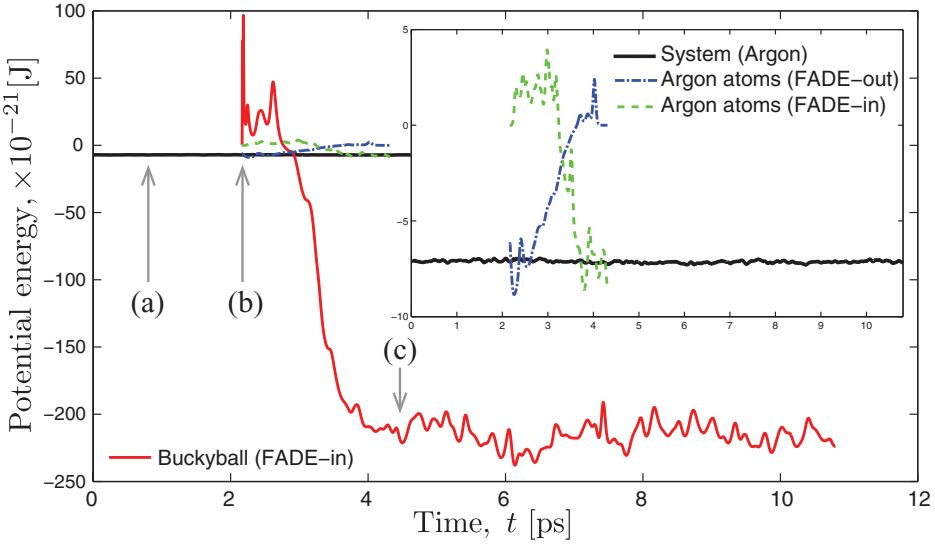

FIG. 16. Potential energy measurements during the insertion of a buckyball in an argon solvent ($N_{Ar} = 3458$ atoms, $T = 293$ K), using the FADE approach with parameters $n = 5$ and $\tau_T = 1000\Delta t$, where $\Delta t = 2.16$ fs. States at (a), (b), and (c), are depicted in Fig. 17.

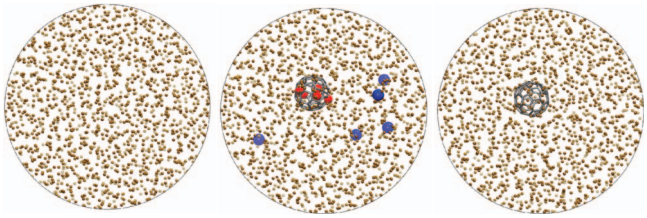

FIG. 17. Snapshots from a periodic cube MD simulation (a) initially filled with argon atoms, (b) FADE-in of buckyball (displayed grey), FADE-out of trapped argon atoms (displayed red) and FADE-in of same atoms returned to bulk (displayed blue), (c) complete insertion of buckyball. Refer also to xs Fig. 16.

re-inserting them back into the bulk solvent using a tandem FADE-in operation, so that solvent mass is conserved. In summary, three FADE operations are happening simultaneously whenever a buckyball is inserted: FADE-in of a buckyball, FADE-out of trapped solvent atoms, and FADE-in of the same number of solvent atoms returned to the bulk.

We consider a periodic cube of side length 5.44 nm that is initially filled with pure argon at $\rho = 1437$ kg/m^3, $T = 292.8$ K, and $N = 3458$ atoms. In Figure 16 we show the potential energy measurements for the insertion of one buckyball, while in Figure 17 we show some representative snapshots. Clearly, the potential energy of the buckyball is much lower than the solvent, which would not be a target insertion site that exists in principle and thus impossible to find using the steepest-descent scheme of the USHER algorithm.[23,47]

Finally we generate pressure-density curves at constant temperature $T = 293$ K, for various constant argon solvent densities. For each case, one buckyball is inserted within the solvent every 4000 MD time steps, of which 1000 time steps are for the FADE, another 1000 for equilibration, and 2000 MD time steps for measurement of pressure. The results of these simulations are presented in Figures 18 and 19.

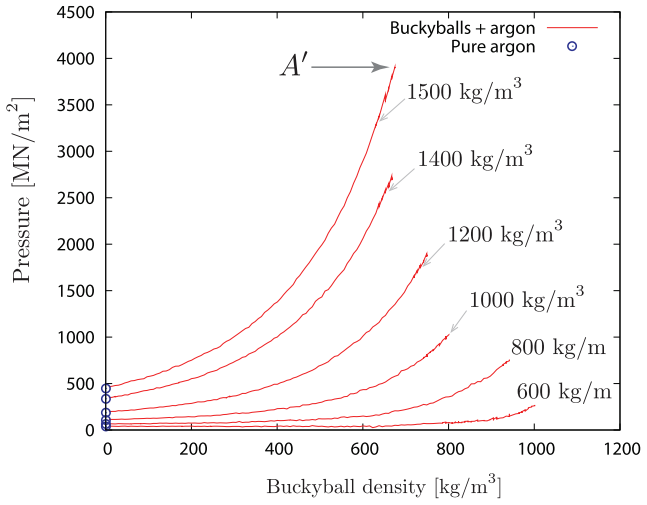

FIG. 18. Isothermal pressure-density curves generated at constant solvent density ρ_{Ar}, for the gradual insertion of buckyballs using FADE. Parameters for FADE are $n = 5$ and $\tau_T = 1000\Delta t$. A snapshot of the MD state at the point marked as A' is displayed in Fig. 19.

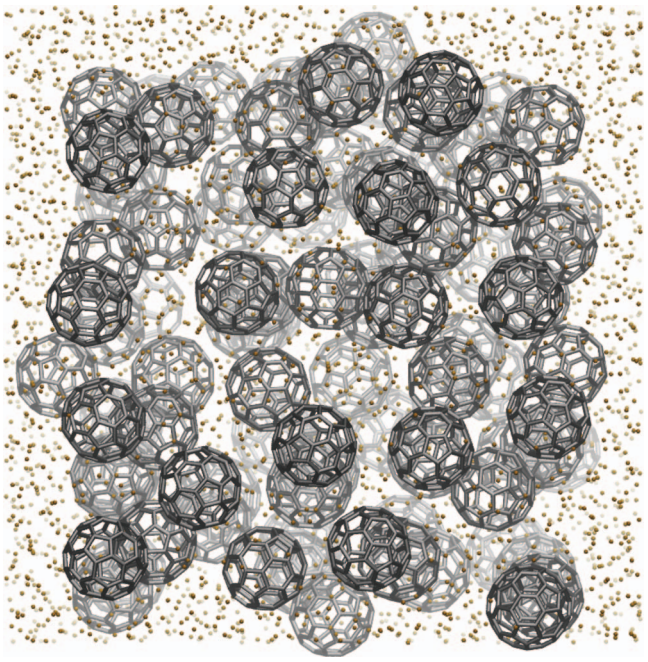

FIG. 19. A snapshot from the MD simulation after the insertion of ~90 buckyballs within an argon solvent of constant density $\rho_{Ar} = 1500$ kg/m^3, taken at point A' indicated in Fig. 18. Note that the individual carbon atoms have been omitted from this diagram for clarity.

IV. CONCLUSIONS

In order to implement open MD systems and hybrid MD-continuum formulations we require the ability to exchange mass, momentum and energy with a surrounding environment. In MD, the insertion of molecules into dense fluids is not a trivial process, mainly because all the fluid molecules are tightly interacting with each other within a complex potential energy field. In this paper we presented a new mass-stat technique called FADE that gradually inserts or deletes molecules at any spatial or temporal point within a MD simulation. Unlike the previous USHER method, which searches iteratively for sites at a target potential energy for inserting molecules, FADE applies a momentum-conserving relaxation of the van der Waals and electrostatic intermolecular bonds, applied by a rational time-weighted function. This means that insertion or deletion occurs over a very short time-scale τ_T, instead of instantaneously (as in USHER). There are many benefits of this approach. First, there is no need for sequential steepest-decent searches of target potential energy sites. The molecules are instead placed randomly or uniformly within the domain, or at sites optimised to account for the locations of existing molecules. The effect of insertion is then progressively felt by neighbouring molecules during the subsequent MD time steps, while the potential energy relaxes gradually to the system environment. FADE is therefore simple to implement in current MD codes and, most importantly, more suitable for a parallel computational implementation; most simulations presented in this paper were run on several processors using a domain decomposition of the MD volume.

We presented monatomic argon and polyatomic TIP4P water simulations to demonstrate a reasonable range of insertion parameters, i.e. the insertion time-scale τ_T, the order of

the polynomial weighting function n, and the insertion ratio $\Delta N/N_0$, that confines spurious energy introduced in the system to within an acceptable level. (This permissible energy variation was taken from the USHER work.)

Quasi-steady MD simulations were then run using FADE and USHER for comparison. Molecules were inserted gradually to generate pressure-density curves at constant temperature. We verified that FADE is at least as computationally efficient and accurate as the USHER approach.

Perhaps the biggest advantage of the FADE algorithm, though, is that it can be applied to insert or delete larger molecules than argon and water. It is not easy to see how this would be possible using USHER. In this paper, we demonstrated this capability by inserting polymer strands of long aspect ratio within polymeric melts, and by inserting hollow carbon fullerenes within a solvent of argon. While the simulations carried out in this work were purely for verification purposes, we have used the USHER algorithm as a basis for validating the FADE mass-stat wherever possible.

In this paper we have not been able to corroborate the MD ensemble of the FADE mass-stat. However, in general non-periodic molecular dynamics and hybrid continuum-MD, insertions/deletions are typically localised within some buffer or constrained region, where the effects of any local perturbation are unnoticeable in the main MD region of interest. The intent of the mass-stat technique was explained through the applications listed in the introduction to this paper, and we propose those studies as future work.

Particle insertions/deletions might also be required where a total chemical potential might need to be maintained such as in extended[14] or control volume GCMD.[18] There are also instances when trial particles are added in order to measure a chemical potential (see for example Ref. 52). The current FADE approach cannot be straightforwardly applied to these problems, and so this will form part of future development.

ACKNOWLEDGMENTS

This work is financially supported in the U.K. by EPSRC Programme, Grant No. EP/I011927/1. Our calculations were performed on the high performance computer ARCHIE at the University of Strathclyde, funded by EPSRC Grant Nos. EP/K000586/1 and EP/K000195/1. We thank the reviewers of this paper for their helpful comments.

[1]M. P. Allen and D. J. Tildesley, *Computer Simulation of Liquids* (Oxford University Press, 1987).
[2]G. Wagner, E. Flekkøy, J. Feder, and T. Jøssang, "Coupling molecular dynamics and continuum dynamics," J. Comput. Phys. Commun. **147**, 670–673 (2002).
[3]R. Delgado-Buscalioni and P. V. Coveney, "Continuum-particle hybrid coupling for mass, momentum, and energy transfers in unsteady fluid flow," Phys. Rev. E **67**, 046704 (2003).
[4]X. B. Nie, S. Y. Chen, W. E, and M. O. Robbins, "A continuum and molecular dynamics hybrid method for micro- and nano-fluid flow," J. Fluid Mech. **500**, 55–64 (2004).
[5]M. K. Borg, G. B. Macpherson, and J. M. Reese, "Controllers for imposing continuum-to-molecular boundary conditions in arbitrary fluid flow geometries," Mol. Simul. **36**, 745–757 (2010).
[6]M. Berkowitz and J. A. McCammon, "Molecular dynamics with stochastic boundary conditions," Chem. Phys. Lett. **90**, 215–217 (1982).
[7]C. L. Brooks III and M. Karplus, "Deformable stochastic boundary conditions in molecular dynamics," J. Chem. Phys. **79**, 6312–6325 (1983).
[8]A. Brunünger, C. L. Brooks III, and M. Karplus, "Stochastic boundary conditions for molecular dynamics of ST2 water," Chem. Phys. Lett. **105**, 495–500 (1984).
[9]P. Attard, "Non-periodic boundary conditions for molecular simulations of condensed matter," Mol. Phys. **104**, 1951–1960 (2006).
[10]T. Werder, J. H. Walther, and P. Koumoutsakos, "Hybrid atomistic-continuum method for the simulation of dense fluid flows," J. Comput. Phys. **205**, 373–390 (2005).
[11]C. L. Brooks III, A. Brünger, and M. Karplus, "Active site dynamics in protein molecules: A stochastic boundary molecular-dynamics approach," Biopolymers **24**, 843–865 (1985).
[12]M. Sun and C. Ebner, "Molecular-dynamics simulation of compressible fluid flow in two-dimensional channels," Phys. Rev. A **46**, 4813–4818 (1992).
[13]W. D. Nicholls, M. K. Borg, D. A. Lockerby, and J. M. Reese, "Water transport through (7,7) carbon nanotubes of different lengths using molecular dynamics," Microfluid. Nanofluid. **12**, 257–264 (2012).
[14]T. Çagin and B. Montgomery Pettitt, "Molecular dynamics with a variable number of molecules," Mol. Phys. **72**, 169–175 (1991).
[15]J. Ji, T. Çagin, and B. Montgomery Pettitt, "Dynamic simulations of water at constant chemical potential," J. Chem. Phys. **96**, 1333–1342 (1992).
[16]R. M. Shroll and D. E. Smith, "Molecular dynamics simulations in the grand canonical ensemble: Formulation of a bias potential for umbrella sampling," J. Chem. Phys. **110**, 8295–9302 (1999).
[17]S. Boinepalli and P. Attard, "Grand canonical molecular dynamics," J. Chem. Phys. **119**, 12769 (2003).
[18]G. S. Heffelfinger and F. van Swol, "Diffusion in Lennard-Jones fluids using dual control volume grand canonical molecular dynamics simulation (DVC-GCMD)," J. Chem. Phys. **100**, 7548–7552 (1994).
[19]J. M. D. MacElroy, "Nonequilibrium molecular dynamics simulation of diffusion and flow in thin microporous membranes," J. Chem. Phys. **101**, 5274–5280 (1994).
[20]A. P. Thompson and G. S. Heffelfinger, "Direct molecular simulation of gradient-driven diffusion of large molecules using constant pressure," J. Chem. Phys. **110**, 10693 (1999).
[21]*Simulation blow-up* occurs when a molecule is inserted within the intermolecular core of one or more existing molecules, which induces a large unrealistic force that bombards all affected molecules into the cores of other molecules in the next time step. This propagates very quickly over a few successive time steps, until the system does not remain homogeneous. It is typically detected when the system potential and kinetic energy measurements are both unphysically large.
[22]J. Cannon, D. Kim, and O. Hess, "The initial flow dynamics of light atoms through carbon nanotubes," Fluid Dyn. Res. **43**, 025507 (2011).
[23]R. Delgado-Buscalioni and P. V. Coveney, "USHER: An algorithm for particle insertion in dense fluids," J. Chem. Phys. **119**, 978–987 (2003).
[24]G. De Fabritiis, R. Delgado-Buscalioni, and P. V. Coveney, "Energy controlled insertion of polar molecules in dense fluids," J. Chem. Phys. **121**, 12139–12142 (2004).
[25]D. C. Rapaport, *The Art of Molecular Dynamics Simulation*, 2nd ed. (Cambridge University Press, 2004).
[26]See www.openfoam.org for OpenFOAM, (2013).
[27]M. K. Borg, D. A. Lockerby, and J. M. Reese, "A multiscale method for micro/nano flows of high aspect ratio," J. Comput. Phys. **233**, 400–413 (2013).
[28]M. K. Borg, D. A. Lockerby, and J. M. Reese, "Fluid simulations with atomistic resolution: a hybrid multiscale method with field-wise coupling," J. Comput. Phys. **255**, 149–165 (2013).
[29]W. D. Nicholls, M. K. Borg, D. A. Lockerby, and J. M. Reese, "Water transport through carbon nanotubes with defects," Mol. Simul. **38**, 781–785 (2012).
[30]K. Ritos, N. Dongari, M. K. Borg, Y. Zhang, and J. M. Reese, "Dynamics of nanoscale droplets on moving surfaces," Langmuir **29**, 6936–6943 (2013).
[31]H. C. Andersen, "Molecular dynamics simulations at constant pressure and/or temperature," J. Chem. Phys. **72**, 2384–2393 (1980).
[32]H. J. C. Berendsen, J. P. M. Postma, W. F. van Gunsteren, A. Dinola, and J. R. Haak, "Molecular dynamics with coupling to an external bath," J. Chem. Phys. **81**, 3684–3690 (1984).
[33]S. T. O'Connell and P. A. Thompson, "Molecular dynamics–continuum hybrid computations: A tool for studying complex fluid flows," Phys. Rev. E **52**, R5792–R5795 (1995).

[34]N. Hadjiconstantinou and A. Patera, "Heterogeneous atomistic-continuum methods for dense fluid systems," Int. J. Mod. Phys. C **08**, 967–976 (1997).
[35]T. Soddemann, B. Dünweg, and K. Kremer, "Dissipative particle dynamics: A useful thermostat for equilibrium and nonequilibrium molecular dynamics simulations," Phys. Rev. E **68**, 046702 (2003).
[36]D. J. Evans and B. L. Holian, "The nose–hoover thermostat," J. Chem. Phys. **83**, 4069 (1985).
[37]C. Junghans, M. Praprotnik, and K. Kremer, "Transport properties controlled by a thermostat: An extended dissipative particle dynamics thermostat," Soft Matter **4**, 156–161 (2008).
[38]The $\tilde{r}_j$ of every atom/molecule can be computed at every time step at negligible additional cost: it involves adding two lines of code inside the intermolecular computation step.
[39]Naturally, thermalisation would be applied simultaneously to remove the heat generated by large insertions.
[40]J. K. Johnson, J. A. Zollweg, and K. E. Gubbins, "The Lennard-Jones equation of state revisited," Mol. Phys. **78**, 591–618 (1993).
[41]G. B. Macpherson and J. M. Reese, "Molecular dynamics in arbitrary geometries: Parallel evaluation of pair forces," Mol. Simul. **34**, 97–115 (2008).
[42]J. L. F. Abascal and C. Vega, "A general purpose model for the condensed phases of water: TIP4P/2005," J. Chem. Phys. **123**, 234505 (2005).
[43]C. Vega and J. L. F. Abascal, "Simulating water with rigid non-polarizable models: a general perspective," Phys. Chem. Chem. Phys. **13**, 19663–19688 (2011).
[44]D. J. Huggins, "Correlations in liquid water for the TIP3P-Ewald, TIP4P-2005, TIP5P-Ewald, and SWM4-NDP models," J. Chem. Phys. **136**, 064518 (2012).
[45]The percentage tolerance is lower in the case of water because the target potential energy, $|U_t|$ is larger in magnitude than that of argon. The excess energy ΔU is kept constant for both argon and water cases.
[46]P. Linstrom and W. Mallard, NIST Chemistry WebBook, NIST Standard Reference Database Number 69 (National Institute of Standards and Technology, Gaithersburg, MD, 2013), see http://webbook.nist.gov.
[47]R. Delgado-Buscalioni, P. Coveney, G. Riley, and R. Ford, "Hybrid molecular-continuum fluid models: implementation within a general coupling framework," Philos. Trans. R. Soc. London **363**, 1975–1985 (2005).
[48]B. Z. Dlugogorski, M. Grmela, and P. J. Carreau, "Viscometric functions for fene and generalized lennard-jones dumbbell liquids in couette flow: molecular dynamics study," J. Non-Newtonian Fluid Mech. **48**, 303–335 (1993).
[49]M. Kröger and S. Hess, "Rheological evidence for a dynamical crossover in polymer melts via nonequilibrium molecular dynamics," Phys. Rev. Lett. **85**, 1128–1131 (2000).
[50]N. Asproulis, M. Kalweit, and D. Drikakis, "A hybrid molecular continuum method using point wise coupling," Adv. Eng. Software **46**, 85–92 (2012).
[51]J. Walther, R. Jaffe, E. Kotsalis, T. Werder, T. Halicioglu, and P. Koumoutsakos, "Hydrophobic hydration of C60 and carbon nanotubes in water," Carbon **42**, 1185–1194 (2004).
[52]B. Widom, "Some topics in the theory of fluids," J. Chem. Phys. **39**, 2808–2812 (1963).